Proceedings of GPPS Forum 18
Global Power and Propulsion Society
Zurich, 10th-12th January 2018
www.gpps.global

GPPS-2018-0064

MECHANICAL DESIGN OF A 3D PRINTED, SEMI-SHROUDED, CENTRIFUGAL COMPRESSOR IMPELLER FOR SUPERCRITICAL CO2 APPLICATION

Fang Li
Hanwha Power Systems
f.li@hanwha.com
Houston, TX, USA

Robert Pelton
Hanwha Power Systems
rob.pelton@hanwha.com
Houston, TX, USA

Sewoong Jung
Hanwha Power Systems
sewoong.jung@hanwha.com
Houston, TX, USA

ABSTRACT

A novel, partially-shrouded centrifugal impeller has been developed which incorporates a self-recirculating casing treatment for improved operation near the critical point in an sCO2 power cycle. This novel impeller design results in unique mechanical design challenges when working to the limits of traditional 2-piece manufacturing. In particular, the semi-shrouded impeller geometry creates a high stress region at the interface of the shroud and the blade tips. Traditional two-piece impeller manufacturing, where the shroud is attached to bladed disk via welding or brazing, results in sharp corner at the weld joint and excessively high stresses. 3D printing was identified as a manufacturing method with sufficient geometric freedom to allow the incorporation of a large filet at the blade/shroud interface to reduce stresses to acceptable levels. A complete structural analysis of the stage was completed and is presented here. The impeller was designed specifically to operate high pressures, and avoid resonances from inlet guide vanes (IGV's) and vanes in the casing treatment cavity. A successful mechanical design was partially demonstrated through scale manufacturing and testing of the stage in air.

INTRODUCTION

A wide-range compressor is particularly valuable for supercritical carbon dioxide (sCO_2) Brayton power cycles which operate near the critical point to reduce the compression work. Near the critical point, small changes of gas conditions including temperature and pressure near the critical point can cause large effects on the compressor aerodynamic performance. Therefore, the compressor needs to design to stably operate over a wide-range of suction conditions.

Compressor operating range, surge limit or stall line, is characterized by the onset of stall at low-flow which can occur in the impeller, diffuser, and/or volute depending on the design of the stage. Various concepts to extend the stall margin have been developed. Variable inlet guide vanes (Steinke and Crouse, 1967) are commonly used to allow turndown at constant pressure, variable position diffuser vanes (William and Huang, 1989; Jian and Whitfield, 1992) to delay the onset of diffuser stall, and passive and active casing treatments (Pinsley et al., 1990; Fisher, 1988; Hunziker, 2001; Sivagnanasundaram et al., 2014) to address inducer stall.

A super-critical CO2 Brayton cycle was proposed as part of US Department of Energy (DOE) Apollo program, to improve the viability of concentrating solar power. A compressor was designed to meet the cycle requirements. Initial aerodynamic assessment showed that the range of the impeller could be improved by adding a self-recirculating casing treatment to the inlet of the compressor. This technique is often applied to open impeller, but at the high pressures in a sCO2 Brayton cycle, covered impellers are required to maximize efficiency.

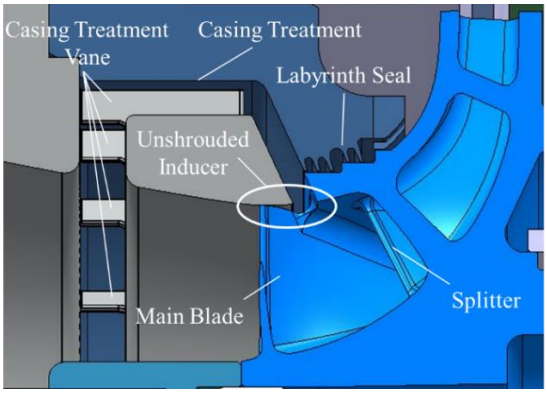

Figure 1 Configuration of Novel Semi-shrouded Impeller with Casing Treatment

In order to integrate a self-recirculating casing treatment with a covered impeller, a novel semi-shrouded impeller was designed for the sCO2 application (Jung and Pelton, 2016;

Pelton et al., 2017). As shown in figure 1, the axial inducer portion of the compressor is unshrouded and interfaces with the stationary casing to create a slot on the shroud where flow can enter or exit the main flowpath. This flowpath opening is connected by a vaned cavity to another slot in the inlet. This allows low momentum fluid in the inducer to recirculate back to inlet which locally increases the flow rate at the inlet and delays the onset of inducer stall. In addition, a number of straight guide vane are included in the cavity to improve performance of the casing treatment.

It is common practice for large covered impellers to be manufactured using a two pieces process. The two pieces are a machined hub with blades and a matching shroud. The shroud is then joined to the bladed disc by one of several processes such as brazing, welding, or a combination of the two. Manufacturing of two piece impellers have the advantage that the individual pieces can be made cost effectively via traditionally 3 or 5 axis milling. Two piece impellers manufactured with this process suffer from several potential issues.

First, the size of the fillet between the blade and the shroud is limited and cannot be very large. Second, the quality of the joint is not consistent and must be carefully inspected on every part. Since the intersection between the blades and the shroud is often a high stress region, the lack of a fillet and uncertain joint quality require substantial margin must be included in the structural design to ensure adequate life. For the semi-shrouded design, it was also found that a significant potential stress concentration at the intersection between the shroud leading edge and the top of the blade. Therefore, it was necessary to identify an appropriate manufacturing option for this type of impeller geometry.

It was initially considered to use a single piece manufactured impeller. Impellers can be made in one piece to avoid the limitation of 2 piece impellers via casting or integral machining. Cast impellers may be a reasonable option for high volume production but are not cost effective for small production orders. Integral machining, where the impeller is machined from a single piece of material, can be very costly and often requires the flowpath geometry to be modified to match the manufacturing limitations. 3D printing has appeared as another option to produce covered impellers which can be cost effective for small production orders and does not typically require flowpath modification to match the process capabilities.

Direct Metal Laser Sintering (DMLS) is 3D printing technique that can build metal parts layer by layer so it is possible to design geometries with challenging internal or complex features that could not be cast or machined. DMLS produces strong, durable parts in a variety kind of alloys including, Ti-6AL-4V, Inconel 718 and stainless steel 17-4 PH, etc. Also with DMLS, materials that are very hard to machined, such as Inconel, can be used widely for little additional cost. Material testing (Gibbin et al., 2016; Emuakpor et al.,2015; Becker et al.,2015) shows that DMLS parts can maintain very good material continuity not only at the bulk material but also at the material transition such as the joint at the shroud and blades. The material test showed that the DMLS parts have both good yield strength and fatigue strength.

MECHANICAL DESIGN CHALLENGES OF TWO-PIECE IMPELLERS

Finite Element Analysis (FEA) on a conventional, fully shrouded compressor was conducted to understand the typical stress distribution in an impeller. External loads including centrifugal load and pressure load were applied to the compressor. The normalized effective stress that defined as the ratio between the effective stresses divided by the maximum effective stress in the impeller, plotted in figure 2, shows that peak stresses develop along the shroud/blade interface. Typical industrial impellers have shown that if the peak stress is kept below 75% of yield, that adequate service life can be achieved. The life is more accurately predicted with a low cycle fatigue analysis, which for this application targets a life of 20 year service. These stress and life calculations assume a perfect joint between the impeller and the blades with the same strength as the base material. Any defect in the shroud joint will reduce the expected life of the impeller and must be quantified and accounted for in the design and manufacture of the stage.

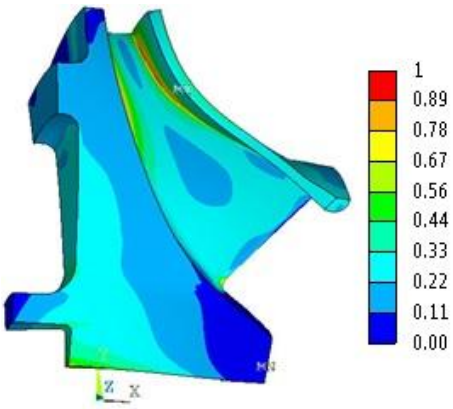

Figure 2 Normalized Effective Stress of a Selected Compressor Impeller

Electron Beam Welding (EBW) was considered as a manufacturing option to give the best joint strength for two-piece impellers. EBW is a thermal joining process that produces a weld by a beam of high energy electrons to heat the joint location and create the weld. A perfect EB welded joint will typically have strength near 100% of the base material, voids or cracks can occasionally be found at the joint leading to high stress concentrations. An example of ultrasonic (UT) inspection of the weld joint on an EBW impeller is shown in figure 3. Incomplete attachment of the shroud to the blades is evident in several locations, see circled regions.

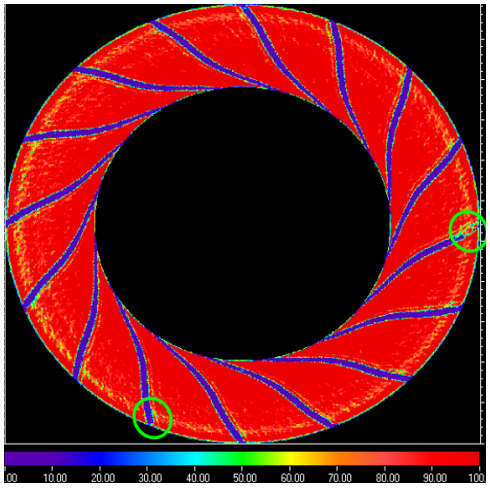

Figure 3 UT scan of the Blade/Shroud Joint on an EBW Compressor Impeller

The voids in the weld joint can be considered as cracks due to their shape, and analysed as such to assess the life of an impeller with an incomplete weld. Based on crack propagation theory, if the crack is bigger than the threshold length, it will grow when subject to dynamic load. The crack thresh hold length, a can be determined using equation (1) (Dowling, N., 2007), where K is the material crack intensity factor, S_g is the stress magnitude, and F is the shape function.

$$a = \frac{K^2}{\pi(FS_g)^2} \quad (1)$$

Based on the stress level and the material fracture toughness, the threshold crack length was found to be around 0.5 mm. And the UT scan shows there are a couple of cracks that are longer than 0.5mm. Thus, the crack growth was expected at the high stress fillets of the compressor. Based on equation (1), the crack intensity factor can be calculated using equation (2).

$$K = FS_g\sqrt{\pi a} \quad (2)$$

From equation (2), crack intensity factor could calculated if the stress and crack length are known. In addition, the crack growth rate can be found using crack growth rate vs. crack intensity factor curves after knowing the crack intensity. Based on the UT scan measurement, the calculated cycles for the cracks to penetrate through the blade and shroud joint for the impeller shown in figure 3 would be about a year, which was matched by the field data.

USING 3D PRINTING TO IMPROVE THE MECHANICAL DESIGN

From equation (2), it can be seen that an EBW impeller/shroud joint is not adequate attachment method if the stress at the joint is high, or the joint cannot be consistently produced free of defects. To avoid these limitations of 2 piece jointed impellers, DMLS 3D printed impellers are considered. Assuming that adequate material properties can be achieved, the process would be well suited for use in high power, high temperature and high pressure applications. To confirm the positive results reported in the literature, tests for DMLS manufactured specimens were conducted independently by Hanwha Power Systems. Test specimens were collected from different sections of a DMLS manufactured compressor impeller. The results showed that the tensile strength of the DMLS material was about 5% higher than the wrought material. Further microstructure test showed the DMLS material has very low porosity and a smaller grain size than the wrought material as seen in figure 4. The finer microstructure of DMLS material may contribute to the improved tensile strength of the DMLS material. Additionally, the microstructure shown in figure 4 (Allison et al., 2014) also demonstrates there are very few porosities in the DMLS material and their size is typically less than 5 µm, which is far below the fracture thresh hold crack length.

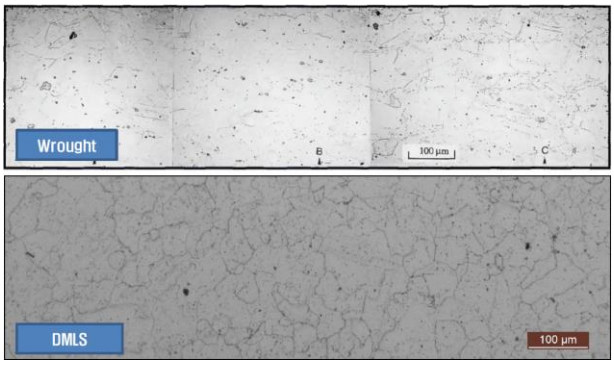

Figure 4 Microstructure of Wrought and DMLS Material

The following characteristics of DMLS make it an attractive method to be used in the high power and loads application.

1. **Expanded geometric design freedom**: 3D printing allows for geometric freedom to reduce the stress level of a DMLS impeller to be much smaller than an EBW part at the same condition. Generally speaking, the peak stress concentration in a shrouded compressor impeller exists at the fillet where the shroud and blade join together. The fillet size of EBW joint is minimal, at only about 0.5mm, which greatly increases the stress concentration factor. For a DMLS impeller a large fillet can be used and the stress concentration factor at the fillet can be much smaller than an EBW compressor.
2. **Good material strength:** Material test shows that DMLS parts maintain consistent density and are free of large voids. Figure 5 (Allison et al., 2014) shows a section cut through a DMLS manufactured compressor, and no void or cracks are evident. Thus, greatly increases the compressor fatigue life comparing an EBW compressor that may have cracks at the joint as shown in figure 3.

Figure 5 Section Cut of DMLS Compressor

3. **Cost effective:** With little additional manufacturing cost, impellers can be produced using materials which is difficult to be machined. For high pressure and high temperature CO2 applications, high corrosion and oxidation resistance are needed. Typically Inconel alloys are used which are usually hard to machine, but easy to print.

DESIGN CONSIDERATION

The cycle that this stage was designed for requires the compressor to operate at discharge pressure around 170 bar. A static structural FEA model was setup to calculate the static state stress to make sure the compressor's maximum stress is below the acceptable level. The impeller was designed to manage both the static loads including the pressure load and centrifugal load and possible dynamic excitations from vanes of casing treatment.

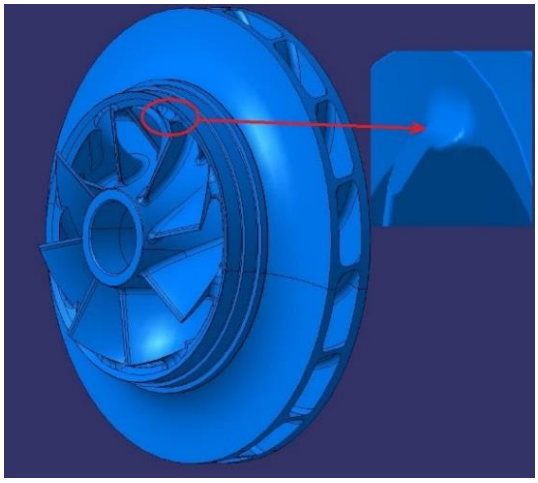

Figure 6 DMLS Impeller with Inducer Unshrouded

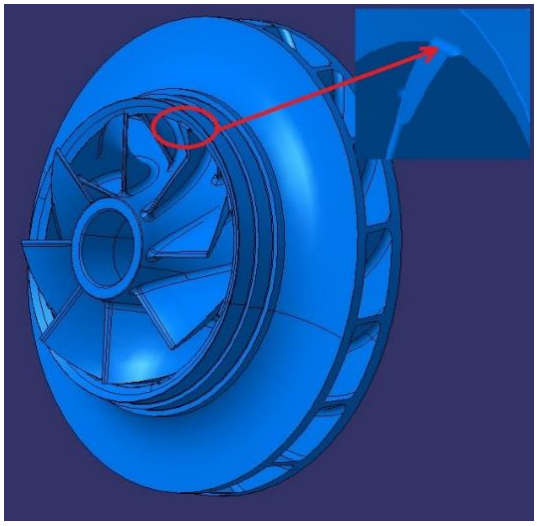

Figure 7 EBW Semi-shrouded Impeller with 0.5mm Fillet Joint

Figure 6 shows the final 3D semi-shrouded impeller model for sCO2 application. The DMLS design incorporates a carefully designed transition between the blade and the shroud leading edge. To reduce the stress level at the joint between the blade and shroud, the size of the fillet is increased to reduce the stress concentration and at the same time, increasing the joint stiffness. It was successfully designed and manufactured via DMLS printing.

As a comparison, the EBW compressor is shown in as figure 7 which has a small 0.5mm fillet. As for the stress induced by the centrifugal load, it can be optimized by reducing the mass at the compressor outer diameter and the compressor hub. The material selection for the compressor is Ti-6AL-4V, which can greatly reduce the stress from centrifugal load comparing to a stainless steel material.

In order to avoid dynamic excitation, the blade thickness at the inducer, where there is no shroud, must be carefully managed to avoid the excitation frequency. In order to have more space to increase the blade thickness of the main blades to avoid dynamic excitation, splitter blades are used as shown in figure 2. The splitter blades are fully covered by the shroud so as to have a high natural frequency to avoid the dynamic excitation.

RESULTS AND DISCUSSION

A FEA was conducted for the compressor using commercial FEA software. A cyclic symmetric model was built by cut one flow path section from the compressor. The pressure load was applied to the cyclic model based on the Computational Fluid Dynamics (CFD) model. The centrifugal load of the compressor also applied to the model based on the maximum operating speed. Figure 8 shows the boundary conditions of the model.

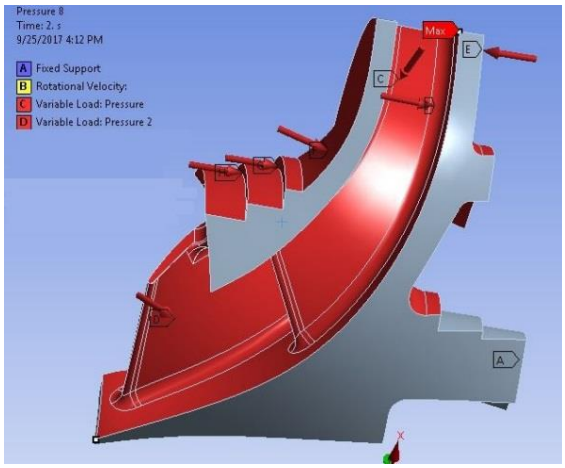

Figure 8 Boundary Conditions of the FEA Model

Two cases were evaluated with the same boundary conditions. First, an EBW type geometry with the shroud/blade fillet limited to 0.5mm. The other case is with 1.7 mm fillets at the "T" joint between the blades and the shroud at the inducer, which is the case of DMLS. For comparison of the effect of different fillets size at the inducer "T" joint, both of the two cases are optimized for centrifugal loads. Both of the two cases have the same main blade thickness to avoid dynamic excitations.

The effective stress of the EBW compressor with 0.5 mm fillets at the inducer of the shroud and blade joint is shown in figure 9. The stress at the inducer fillet of the shroud and blade joint is 990 MPa, or 116% of yield, with very high stress concentration and fails to meet acceptable design criterion.

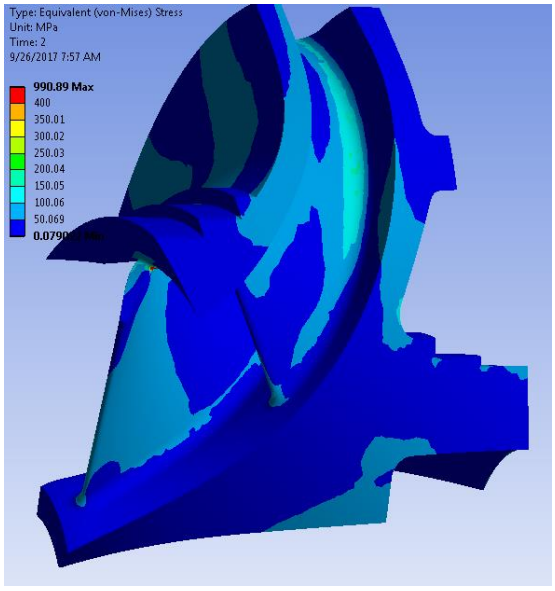

Figure 9 Effective Stress of EBW Impeller

The effective stress of the DMLS compressor with 1.7 mm fillets at the inducer of the shroud and blade joint is shown in figure 10. With the increased fillet, the maximum effective stress is reduced to 271 MPa, or just 32% of yield, which occurs at the same location as the EBW compressor. The bigger fillet at the blade and shroud joint not only reduces the stress concertation factor but also increases the bending stiffness of the joint, thus greatly reduced the effective stress at the join comparing to the EBW compressor.

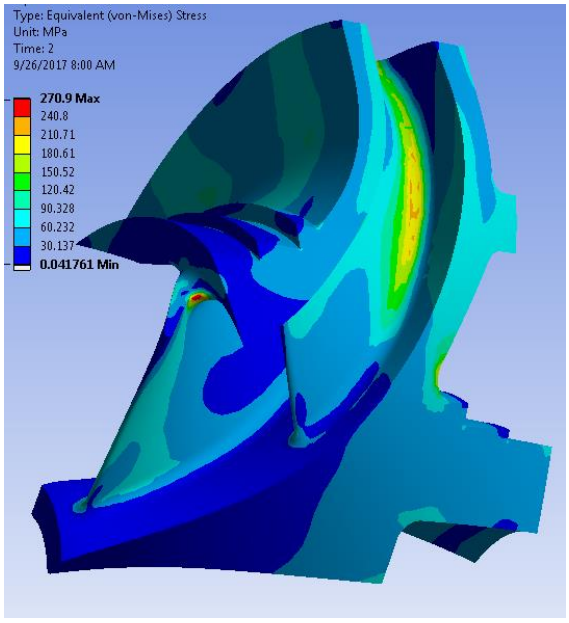

Figure 10 Effective Stress of DMLS Impeller

To ensure that the impeller avoids dynamic excitation from the stationary vanes of the casing treatment, Singh's Advanced Frequency Evaluation (SAFE) diagram is used to examine possible interference between the excitation frequency and the compressor natural frequency. (Bertini et al., 2016; Wang et al., 1999) To evaluate the natural frequencies of the compressor, a pre-stress modal analysis was conducted right after the static structural analysis. The compressor is designed to avoid the first four engine order excitations. The first blade mode of the compressor is shown as in figure 11. The natural frequency is more than 15,000 Hz, which is much higher than the 4th engine order frequency at around 2,000 Hz.

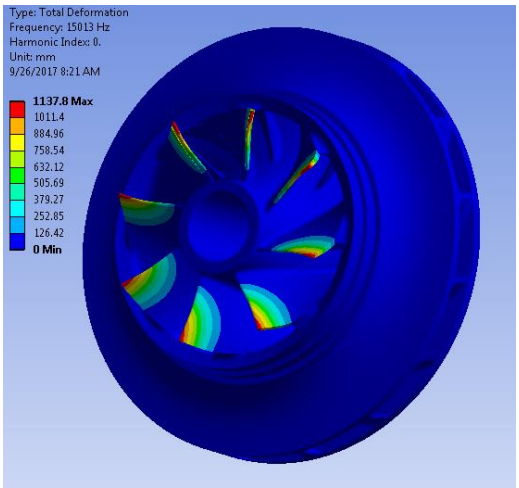

Figure 11 The First Inducer Blade Mode of DMLS Impeller

The SAFE diagram is created based on the excitation and compressor natural frequency, shown as in figure 12. The compressor has eight cyclic symmetric sections, thus there are 4 nodal lines in the SAFE diagram. It can be seen that the first blade mode is at 15,000 Hz. There are two disk modes under the first blade mode and they are all higher than 5,000 Hz, which is above the 10th engine order. The current casing treatment vane count selection is 21, as shown in figure 10. It can be seen from the SAFE diagram that all the compressor modes has large separation margin from 21 vane excitation frequency. Thus, it is a robust design by using 21 vanes for the casing treatment at the aspect of dynamic excitation to the compressor.

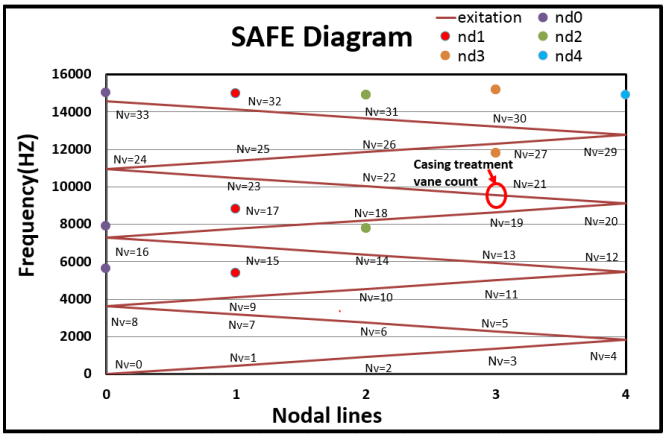

Figure 12 SAFE Diagram of DMLS Impeller

The optimized impeller geometry was printed in IN 625 for shop testing. Figure 13 shows the final printed and machined impeller. Care was taken during final machining to ensure a smooth transition from the machined surfaces to the printed flowpath at the shroud leading edge interface with the blade where the peak stress is predicted. Before testing the impeller was inspected and over speed tested to 115% of running speed. The impeller was subsequently tested in air, at full speed and has accumulated about 40 hrs of operation.

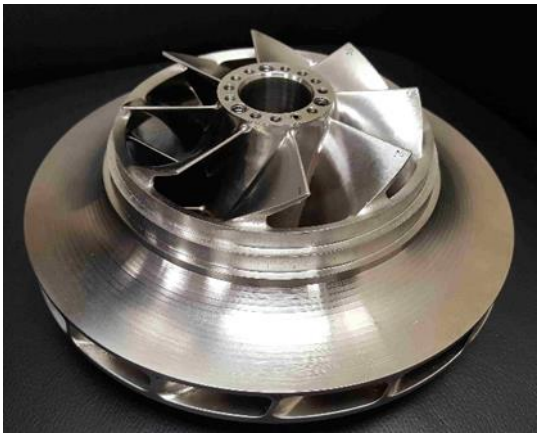

Figure 13 3D Printed Semi-shrouded Compressor Impeller

CONCLUSIONS

A semi-shrouded impeller has a unique mechanical design was developed. The semi-shrouded design has an interface between the leading edge of the shroud and the blade tip that leads to a potentially large stress concentration that is unique to this style compressor. EBW was shown not to be a viable manufacturing process for this type of impeller since only a small fillet can be created at the blade/shroud joint. Additionally, potential imperfections in the EBW joint further reduce the expected life of a two-piece impeller.

A 3D printable impeller geometry was developed to improve the structural characteristic of the stage. DMLS provides the geometry freedom to optimize the compressor to reduce the stress concentration and increase structural stiffness to reduce the stress level. For the DMLS compressor designed by Hanwha Power Systems, the maximum stress was reduced to less than 1/3 of the stress in an EBW compressor at the same condition. 3D printing was demonstrated to produce a material with microstructure free of major voids or cracks, yielding much better material continuity at the high stress regions near the shroud than can be achieved with EBW. Therefore 3D printing has enabled production of novel semi-shrouded impeller geometry that could not be designed with adequate strength using traditional 2-piece manufacturing methods. This result demonstrate that DMLS can provide a feasible solution for the shrouded compressors under high load conditions, such as sCO2 with high pressure and high temperature, where an EBW compressor could encounter excessive stress due to its geometry limitation.

NOMENCLATURE

a: Crack thresh hold length
K: Material crack intensity factor
S_g: Stress magnitude
F: Shape function

ACRONYMS

IGV's:	inlet guide vanes
$sCO_{2:}$	supercritical carbon dioxide
DOE:	US Department of Energy
DMLS:	direct Metal Laser Sintering
EBW:	electron Beam Welding
UT:	ultrasonic
FEA:	finite element analysis

ACKNOWLEGEMENTS

This material is based upon work supported by the Department of Energy, Office of Energy Efficiency and Renewable Energy (EERE), under Award Number DE-0007114.

DISCLAIMER

This report was prepared as an account of work sponsored by an agency of the United States Government. Neither the United States Government nor any agency thereof, nor any of their employees, makes any warranty,

express or Implied, or assumes any legal liability or responsibility for the accuracy, completeness, or usefulness of any information, apparatus, product, or process disclosed, or represents that its use would not infringe privately owned rights. Reference herein to any specific commercial product, process, or service by trade name, trademark, manufacturer, or otherwise does not necessarily constitute or imply its endorsement, recommendation, or favoring by the United States Government or any agency thereof. The views and opinions of authors expressed herein do not necessarily state or reflect those of the United States Government or any agency thereof.

REFERENCES

[1] Allison, T., Moore, J., Rimpel, A., Wilkes, J., Pelton, R., Wygant, K., 2014, "Manufacturing and testing experience with Direct Metal Laser Sintering for Closed Centrifugal Compressor Impellers," 43rd Turbomachinery & 30th Pump Users Symposia (Pump & Turbo 2014), September 23-25, 2014,

[2] Becker, T., Beck, M. and Scheffer, C., 2015. "Microstructure and Mechanical Properties of Direct Metal Laser Sintered Ti-6AL-4V", South African Journal of Industrial Engineering, Vol 26(1), pp 1-10

[3] Bertinia, L., Neria, P., Santusa, C., Guglielmob, A., and Mariotti, G., 2013. "Explanation and Application of the SAFE Diagram" Journal of Sound and Vibration RASD 2013-11

[4] Dowling N.,2007. "Mechanical Behavior of Material", 3rd edition, Pearson Prentice Hall.

[5] Emuakpor, S., Schwartz, J., George, T., Holycross, C., Cross, C., and Slater, J., 2015. "Bending fatigue Life Characterization of Direct Metal Laser Sintering Nickel Alloy 718". Fatigue & Fracture of Engineering Materials & Structures, 38, pp 1105-1117

[6] Fisher, F.B., 1988. "Application of Map Width Enhancement Devices to Turbocharger Compressor Stage", Society of Automotive Engineers, Paper No. 880794

[7] Hunziker, R., Dickmann, H-P., and Emmrich, R., 2001. "Numerical and Experimental Investigation of a Centrifugal Compressor with an Inducer Casing Bleed System", Proc IMechE Part A: J Power and Energy, 215(6) 783-791

[8] Jian, P.M. and Whitfield, A., 1992. "Investigation of Vaned Diffuser as A Variable Geometry Device for Application to Turbocharger Compressors", Proc iMeche Instn. Mech. Engrs. Vol.206, pp209-220.

[9] Jung, S. and Pelton R., 2016. "Numerically Derived Design Guidelines of Self Recirculation Casing Treatment for Industrial Centrifugal Compressors", ASME GT2016-56672

[10] Pinsley, J. E., Guenette, G. R., Epstein, A. H. and Greitzer, E. M., 1990. "Active stabilization of centrifugal compressor surge" ASME paper 90-GT-123

[11] Pelton, R., Jung, S., Allison, T., and Smith, N., 2017. "Design of a Wide-Range Centrifugal Compressor Stage for Supercritical CO2 Power Cycle", GT2017-65172

[12] Sivagnanasundaram, S., Spence, S., Early, J., 2014, "Map Width Enhancement Technique for a Turbocharger Compressor" Journal of Turbomachinery, Vol. 136, No. 6, pp. 061002-1-10

[13] Sribbin, S., Bicknell, J., Jorgensen, L., Tsukrov, I., and Knezevic, M., 2016. "Low Cycle Fatigue Behavior of Direct Metal Laser Sintered Inconel Alloy 718", International Journal of Fatigue, 93, pp 156-167

[14] Steinke, R.J. and Crouse, J.E., 1967. "Preliminary Analysis of the Effectiveness of Variable Geometry Guide Vanes to Control Rotor-inlet Flow Conditions", NASA TN-D 3823

[15] Wang, Q., Bartos, J. and Houston, R., 1999. "Methodology of Open Bladed Impeller Resonance Identification", Proceedings of the 28th Turbomachinery Symposium, pp 61-68

[16] Williams, J. F. and Huang, X., 1989. "Active Stabilization of Compressor Surge", Journal of fluid Mechanics, Vol.204, pp 245–262